JOURNAL OF AIRCRAFT
Vol. 32, No. 2, March–April 1995

Acoustic Spinning-Mode Analysis by an Iterative Threshold Method

Daniel Blacodon*
ONERA, 92322 Châtillon, France

Spinning-mode analysis methods are commonly used for studying the spatial structure of the acoustic field inside ducts. In some applications, the background noise is very high, so that the acoustic modes may be overwhelmed by spurious modes in the modal spectra. The problem may be solved by methods that greatly reduce the background noise. Four methods studied in a previous work are briefly summarized in this article. The method providing the best reduction of the background noise is inaccurate in certain cases. An iterative threshold technique is proposed to eliminate this drawback. It is compared to the four other methods using numerical simulations and mode measurements in the nozzle of a Turbomeca TM333 turboshaft engine.

Nomenclature

f = frequency
G_i = gain in signal to noise ratio of method $i = 10\log[(S/N)_{OUT}/(S/N)_{IN}]$
I = unit matrix
$\mathrm{Im}[\omega(f, m)]$ = imaginary part of $\omega(f, m)$
J = number of microphones
L = number of data blocks
M_N = set of noise modes
M_S = set of acoustic modes, signal
m = angular wave number of spinning mode order
$N(f, \theta)$ = frequency Fourier transform of $n(t, \theta)$
$n(t, \theta)$ = background noise
$\mathrm{Re}[\omega(f, m)]$ = real part of $\omega(f, m)$
$S(f, \theta)$ = frequency Fourier transform of $s(t, \theta)$
$s(t, \theta)$ = acoustic pressure, signal
$T_{S\min}$ = the smallest power spectral density on a noise mode
$Tr[\Gamma(f)]$ = trace of matrix $\Gamma(f)$
t = time
$Y(f, \theta)$ = frequency Fourier transform of $y(t, \theta)$
$y(t, \theta)$ = time history of acoustic pressure (signal + noise) measured by a microphone at angle θ
$\Gamma_N(f)$ = cross-spectral matrix of $N(f, \theta)$
$\Gamma_S(f)$ = cross-spectral matrix of $S(f, \theta)$
$\Gamma_Y(f)$ = cross-spectral matrix of $Y(f, \theta)$, see Eq. (3)
δ = Kronecker symbol
θ = angle
θ_j = location angle of microphone $j\,[=2\pi(j-1)/J]$, $j = 1, 2, \ldots, J$
$\sigma^2(f)$ = noise power spectral density
$\Phi_i(f, m)$ = wave number spectrum at frequency f by method i
$\omega(f, m)$ = angular Fourier transform of $Y(f, \theta)$
$*$ = complex conjugate
$+$ = transposed complex conjugate

Presented as Paper 92-02-041 at the AIAA 14th Aeroacoustics Conference, Aachen, Germany, May 11–14, 1992; received Dec. 11, 1992; revision received June 17, 1994; accepted for publication July 1, 1994.

*Research Scientist, Physics Department, BP 72. Member AIAA.

I. Introduction

THE spinning mode analysis of an acoustic field is a powerful means for getting a better understanding of noise sources in turboshaft engines. It is also the main information needed to predict the far-field directivity radiated from the inlet or nozzle. A spinning mode is defined by two integer numbers, the angular wave number m, and the radial index. The article focuses on the angular wave number spectrum for two reasons:

1) Only the values of m are determined by the symmetries of the sources, sound radiation can be reduced by acting on them by generating decaying acoustic wave in the duct.

2) The application shown in 1 deals with transonic turbines. In this case, a shaft-rotation harmonic is dominated by the value of m equal to the harmonic order, and only the first radial mode can generally propagate.

Angular wave number spectra (spinning mode distributions) have been measured for several years in turbofan engines using a rotating microphone along with a fixed microphone that provided a phase reference.[1-3] This kind of device cannot usually be fitted in turboshaft engines because of their small size and also because the duct cross section may not be perfectly circular. Another approach uses an array of fixed microphones around the duct. However, two main difficulties appear with this technique. The first limitation is due to the spatial sampling of the sound field. According to the Nyquist's criterion, the number of microphones must be at least twice as high as the highest spinning mode in the acoustic field. The second difficulty arises if the background noise is high. Some actual spinning modes may be overwhelmed by spurious modes. A suitable method to improve the signal to noise ratio (S/N) is needed. The gains in (S/N) of several methods have been compared in a previous work using numerical simulations and mode measurements in a nozzle of a Turbomeca engine.[4]

The aim of this article is to derive a new analysis technique from method 4 in order to solve the above problem. The article begins with a brief theoretical review of methods 1–4 (Sec. II). Section III is devoted to the description of a threshold method (method 5). It adds coherently the cross spectral matrix terms due to the acoustic field, and incoherently those due to the background noise terms. The drawback of method 4 is thus suppressed. It is well known that the quality of the results provided by a threshold method depends on the criterion chosen for the definition of an appropriate threshold. The calculation of an optimum threshold by an iterative technique (method 6) is also proposed in Sec. III. The six methods are compared by numerical simulations in Sec. IV.

Tests were performed in May 1986 in the Turbomeca outdoor facility at Pau-Uzein. A cross section of a TM333 tur-

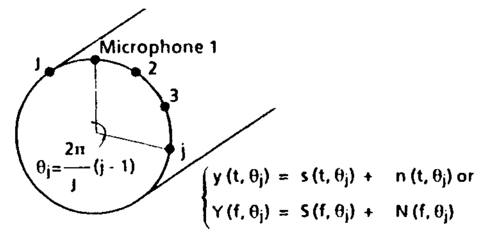

Fig. 1 Array of fixed equidistant microphones for spinning modes analysis.

boshaft engine nozzle was equipped with eight flush-mounted probes, every 45 deg. The results obtained with methods 1, 2, 3, and 6 are presented in Sec. V.

II. Theoretical Background

The four methods studied in Ref. 4 are based on the cross-spectral matrix of the measured signals. The calculation of this matrix and a short theoretical background of these methods are presented in this section.

A. Cross-Spectral Matrix

Measurements are made using an array of J fixed microphones flush-mounted on the wall of a cylindrical duct cross section, as shown in Fig. 1. The time signal $y(t, \theta_j)$ measured by a microphone at angle θ_j is written

$$y(t, \theta_j) = s(t, \theta_j) + n(t, \theta_j) \tag{1}$$

The Fourier transform in the frequency domain is

$$Y(f, \theta_j) = S(f, \theta_j) + N(f, \theta_j) \tag{2}$$

A subscript l should be introduced in all the above notations because the Fourier transforms are computed on data block intervals $(l - 1)T < T < lT$ $(l = 1$ to $L)$, where T is greater than the maximum period under study (the frequency resolution is $\Delta f = 1/T$)

Let us consider the column matrix

$$\boldsymbol{Y}_l(f) = \begin{bmatrix} Y_l(f, \theta_1) \\ Y_l(f, \theta_2) \\ \vdots \\ Y_l(f, \theta_J) \end{bmatrix}$$

$\boldsymbol{Y}_l(f)$ is assumed to be stationary. The cross-spectral matrix of $\boldsymbol{Y}_l(f)$ is evaluated by performing a statistical average on L data blocks:

$$\Gamma_Y(f) = \langle \boldsymbol{Y}_l(f) \cdot \boldsymbol{Y}_l^+(f) \rangle = \lim_{L \to \infty} \frac{1}{L} \sum_{l=1}^{L} \boldsymbol{Y}_l(f) \cdot \boldsymbol{Y}_l^+(f) \tag{3}$$

B. Methods 1 and 2

Method 1 is conventional for computing the angular wave number spectra from $\Gamma_Y(f)$. The wave number spectrum at f is given by

$$\Phi_1(f, m) = \boldsymbol{U}^+ \cdot \Gamma_Y(f) \cdot \boldsymbol{U}, \quad \text{with } \boldsymbol{U} = \frac{1}{J} \begin{bmatrix} \exp(im\theta_1) \\ \exp(im\theta_2) \\ \vdots \\ \exp(im\theta_J) \end{bmatrix} \tag{4}$$

Two general hypotheses are assumed to determine the gain in (S/N) of the method: 1) the background noise on the microphones is uncorrelated with the acoustic field:

$$\langle S_l(f, \theta_j) \cdot N_l^*(f, \theta_{j'}) \rangle = 0 \tag{5}$$

2) the background noises at two different angles are also uncorrelated. This means that the spacing between microphones is sufficiently large:

$$\langle N_l(f, \theta_j) \cdot N_l^*(f, \theta_{j'}) \rangle = \sigma^2(f) \cdot \delta_{jj'} \tag{6}$$

Taking these two hypotheses into account, the cross-spectral matrix is written

$$\Gamma_Y(f) = \Gamma_S(f) + \Phi_N(f) \tag{7}$$

where

$$\Gamma_S(f) = \langle \boldsymbol{S}_l(f) \cdot \boldsymbol{S}_l^+(f) \rangle, \quad \text{with } \boldsymbol{S}_l(f) = \begin{bmatrix} S_l(f, \theta_1) \\ S_l(f, \theta_2) \\ \vdots \\ S_l(f, \theta_J) \end{bmatrix}$$

and $\Gamma_N(f) = [\sigma^2(f) \cdot I]$ is a diagonal noise matrix. The input (S/N) is

$$(\mathrm{S/N})_{\mathrm{IN}} = Tr[\Gamma_S(f)]/Tr\Gamma_N(f)] = \sum_{j=1}^{J} S_{jj}(f) \Big/ J\sigma^2(f) \tag{8}$$

where

$$S_{jj}(f) = \langle S_l(f, \theta_j) \cdot S_l^*(f, \theta_j) \rangle$$

After data processing, the output (S/N) is

$$(\mathrm{S/N})_{\mathrm{OUT}} = \frac{\Phi_S(f, m)}{\Phi_N(f, m)} = \frac{\langle |S_l(f, m)|^2 \rangle}{[\sigma^2(f)/J^2]} \tag{9}$$

The gain in (S/N) is defined as

$$G_1(f, m) = (\mathrm{S/N})_{\mathrm{OUT}}/(\mathrm{S/N})_{\mathrm{IN}} \tag{10}$$

If there is a single mode m_0 in the acoustic pressure, then

$$\sum_{j=1}^{J} S_{jj}(f) = J \langle |S_l(f, m_0)|^2 \rangle_J \tag{11}$$

$$G_1 = J \text{ or } G_1\ (\mathrm{dB}) = 10 \log G_1 = 10 \log J \tag{12}$$

This relation shows that the gain in (S/N) depends only on J. Large arrays are faced with complex technical problems: ducts of small size, signal conditioning, calibration, and recording. Thus, J is generally small, so that a large background noise reduction cannot be achieved. As a consequence, this method is not suitable for the modal analysis of a very noisy acoustic field.

The relation [Eq. (7)] shows that the background noise terms are only diagonal. The limitation in gain G_1 is in fact due to these terms, and any improvement in the gain G_1 requires the removal of the additive noise power spectral density (PSD) $\sigma_j^2(f)$ $(j = 1, 2, \ldots, J)$ in $\Gamma_Y(f)$. This may be achieved by a three signal-coherence technique.[5,6] Let us consider the signals measured at angles θ_j, θ_k, θ_n:

$$Y_l(f, \theta) = S_l(f, \theta) + N_l(f, \theta) \text{ for } \theta = \theta_j, \theta_k \text{ and } \theta_n$$

The coherent diagonal term j of the cross-spectral matrix is

$$Y_{jj}^c(f) = \frac{Y_{jk}(f) \cdot Y_{nj}(f)}{Y_{nk}(f)} \tag{13}$$

where

$$Y_{\nu\nu'}(f) = \langle Y_l(f, \theta_\nu) \cdot Y_l^*(f, \theta_{\nu'}) \rangle \tag{14}$$

Taking into account the hypotheses (5) and (6), Eq. (13) can be written

$$Y_{jj}^{c}(f) = \frac{S_{jk}(f)\cdot S_{nj}(f)}{S_{nk}(f)} \tag{15}$$

Background noise is clearly removed. $Y_{jj}(f)$ ($j = 1, 2, \ldots, J$) is replaced by $Y_{jj}^{c}(f)$ on the diagonal of $\Gamma_Y(f)$. We obtain a new matrix $\Gamma_Y^c(f)$ without the noise terms. This is used in method 2:

$$\Phi_2(f, m) = \boldsymbol{U}^{+}\cdot\Gamma_Y^c(f)\cdot\boldsymbol{U} \tag{16}$$

This method would be perfect if the actual cross-spectral matrix were known (i.e., computed on an infinite number of data blocks). In practice, it is estimated by

$$\hat{\Gamma}_Y(f) = \langle \boldsymbol{Y}_l(f)\cdot\boldsymbol{Y}_l^{+}(f)\rangle_L = \frac{1}{L}\sum_{l=1}^{L}\boldsymbol{Y}_l(f)\cdot\boldsymbol{Y}_l^{+}(f) \tag{17}$$

i.e., by computing Eq. (3) with a finite number L of data blocks. In this case, Eqs. (5) and (6) are not strictly valid, and $\Gamma_Y(f)$ contains diagonal and nondiagonal noise terms. These nondiagonal terms are due to an estimation error in the cross-spectral components $Y_{jj'}(f)$. The variance of $Y_{jj'}(f)$ is given by

$$\sigma_Y^2(f) = \langle|\hat{Y}_{jj'}(f) - Y_{jj'}(f)|^2\rangle = \sigma^2(f)/\sqrt{L} \tag{18}$$

It appears that the error decreases as $\sqrt{L}$ increases. The estimation errors are similar to those in $Y_{jj'}(f)$, since $Y_{jj}^{c}(f)$ is deduced from the $Y_{jj'}(f)$. The noise PSD is thus divided by $\sqrt{L}$. Thus, this attractive method provides an improvement in (S/N) gain only equal to

$$G_2\,(\mathrm{dB}) = G_1\,(\mathrm{dB}) + 10\log\sqrt{L} = 10\log(J\sqrt{L}) \tag{19}$$

As a consequence, the gain G_2 is only slightly increased, even for a large value of L.

C. Methods 3 and 4

The nondiagonal noise terms of the matrix, which were previously negligible, become predominant since the noise PSDs $\sigma_j^2(f)$ ($j = 1, 2, \ldots, J$) have been removed in the $\Gamma_Y^c(f)$ formula. These residual noise terms must now be reduced to further improve the gain G_2. This is a simple way of achieving this.

Let us first modify each line of $\Gamma_Y^c(f)$ in order to obtain a new matrix:

$$\Gamma_W(f) = \begin{bmatrix} \boldsymbol{W}_1(f) \\ \boldsymbol{W}_2(f) \\ \vdots \\ \boldsymbol{W}_J(f) \end{bmatrix}$$

where the line vector $\boldsymbol{W}_j(f)$ corresponds to the angular evolution of the cross-spectral densities computed between a reference signal at angle $\theta_j = 2\pi(j-1)/J$, and the other signals at locations $\varphi_k = \theta_k - \theta_j$ ($k = j+1, \ldots, J+j-1$).

The wave number spectrum can be calculated with any of line vector of $\Gamma_W(f)$[1-3] using the following relation:

$$\Phi_3^j(f, m) = |\boldsymbol{U}^{+}\cdot\boldsymbol{W}_j(f)|^2/\hat{Y}_{jj}^{c}(f) \tag{20}$$

This is similar to the data processing technique using a fixed and a moving microphone. The gain in (S/N), G_3, for method 3 is limited by the errors in the estimation of the cross-spectral densities. As a consequence, G_3 is of the same order as G_2.

The coherence features of the acoustic field can now be used to reduce the residual noise in $\Gamma_W(f)$ by averaging the terms in each of its columns:

$$\langle\boldsymbol{W}(f)\rangle_J = \frac{1}{J}\sum_{j=1}^{J}\frac{\boldsymbol{W}_j(f)}{\sqrt{\hat{Y}_{jj}^{c}(f)}} \tag{21}$$

This provides a reduction of the noise variance by a factor J. Method 4 leads to

$$\Phi_4\,(f, m) = |\boldsymbol{U}^{+}\cdot\langle\boldsymbol{W}(f)\rangle_J|^2 \tag{22}$$

Its gain in (S/N) is the highest one:

$$G_4(\mathrm{dB}) = 10\log(J^2\sqrt{L}) \tag{23}$$

However, method 4 has a major drawback. It is able to characterize quantitatively only the acoustic modes whose terms are in phase in each column of the matrix $\Gamma_W(f)$. The amplitudes of the other acoustic modes are more or less underpredicted, their terms being averaged incoherently in $\langle\boldsymbol{W}(f)\rangle_J$. In other words, these modes are not processed as signal, but as noise.

III. Threshold Modal Analysis Methods

A. Need for a Threshold Method

As explained above, the drawback of method 4 arises in the calculation of the line matrix $\langle\boldsymbol{W}(f)\rangle_J$. Thus, the acoustic terms must be put in phase in each column of $\Gamma_W(f)$ before calculating $\langle\boldsymbol{W}(f)\rangle_J$. This operation cannot be carried out without the knowledge of the acoustic terms in each vector $\boldsymbol{W}_j(f)$ of $\Gamma_W(f)$. There is no simple means to separate the acoustic and noise terms in the $\boldsymbol{W}_j(f)$ vectors, and it remains difficult to overcome the drawback of method 4.

Let us first define the following matrix:

$$\Psi(f, m) = \begin{bmatrix} \boldsymbol{\omega}_1(f, m) \\ \boldsymbol{\omega}_2(f, m) \\ \vdots \\ \boldsymbol{\omega}_J(f, m) \end{bmatrix}$$

where

$$\boldsymbol{\omega}_j(f, m) = \boldsymbol{U}^{+}\cdot\boldsymbol{W}_j(f)/\sqrt{Y_{jj}^{c}} \tag{24}$$

denotes the angular Fourier transform of the normalized line vector $\boldsymbol{W}_j(f)$ of $\Gamma_W(f)$. Equation (20) becomes

$$\Phi_{3'}^{j}(f, m) = |\boldsymbol{\omega}_j(f, m)|^2 \tag{25}$$

Method 4′ yields

$$\Phi_{4'}(f, m) = |\langle\boldsymbol{\omega}(f, m)\rangle_J|^2, \qquad \langle\boldsymbol{\omega}(f, m)\rangle_J = \frac{1}{J}\sum_{j=1}^{J}\boldsymbol{\omega}_j(f, m) \tag{26}$$

Due to the linearity of the Fourier transform

$$\Phi_4(f, m) = \Phi_{4'}(f, m) \tag{27}$$

It is clear that the problem encountered in method 4 for the calculation of $\langle\boldsymbol{W}(f)\rangle_J$ [see after Eq. (23)] also appears when computing $\langle\boldsymbol{\omega}(f, m)\rangle_J$. The acoustic terms that are not in phase in the columns of $\Psi(f, m)$ are incoherently averaged in $\langle\boldsymbol{\omega}(f, m)\rangle_J$. However, it is now possible to separate the acoustic and noise terms in the vectors $\boldsymbol{\omega}_j(f, m)$ ($j = 1, 2,$

$\ldots, J$). More precisely, each vector $\boldsymbol{\omega}_j(f, m)$ [Eq. (2)] can be split into two vectors:

$$\boldsymbol{\omega}_j(f, m) = \begin{cases} \boldsymbol{\omega}_j^S(f, m) \text{ for } m \in M_S \text{ (acoustic vector)} \\ \boldsymbol{\omega}_j^N(f, m) \text{ for } m \in M_N \text{ (noise vector)} \end{cases} \quad (28)$$

The coherent addition of the acoustic terms and the incoherent addition of the noise terms may be then done by calculating

$$\langle \boldsymbol{\omega}'(f, m) \rangle_J = \frac{1}{J} \sum_{j=1}^{J} \boldsymbol{\omega}_j'(f, m) \quad (29)$$

with

$$\boldsymbol{\omega}_j'(f, m) = \begin{cases} |\mathrm{Re}[\boldsymbol{\omega}_j^S(f, m)]| + i|\mathrm{Im}[\boldsymbol{\omega}_j^S(f, m)]| \text{ for } m \in M_S \\ \boldsymbol{\omega}_j^N(f, m) \text{ for } m \in M_N \end{cases}$$

It must be noticed that the real and imaginary parts of the vector $\boldsymbol{\omega}_j^S(f, m)$ are positive since they are absolute values. As a consequence, they are coherently added in $\langle \boldsymbol{\omega}'(f, m) \rangle_J$. On the contrary, noise terms are incoherently added in $\langle \boldsymbol{\omega}'(f, m) \rangle_J$ as the real and the imaginary parts of these components do not have the same sign in each $\boldsymbol{\omega}_j^N(f, m)$ vector.

B. Hypotheses

One of the two sets M_S or M_N must be found to calculate the line matrix $\langle \boldsymbol{\omega}'(f, m) \rangle_J$. This can be achieved by a threshold method. It is based on three hypotheses concerning the amplitudes of the acoustic and of the noise modes.

Hypothesis 1: The amplitudes of the acoustic modes are assumed to be deterministic. They are correctly predicted by method 3 [Eq. (25)] with any $\boldsymbol{\omega}_j(f, m)$ vector of $\Psi(f, m)$:

$$\forall\, m \in M_S, \forall\, j, j', |\boldsymbol{\omega}_j(f, m)|^2 = |\boldsymbol{\omega}_{j'}(f, m)|^2 \quad (30)$$

This relation allows to write

$$\forall\, m \in M_S, \forall\, j, |\boldsymbol{\omega}_j(f, m)|^2 = \langle |\boldsymbol{\omega}(f, m)|^2 \rangle_J \quad (31)$$

where

$$\langle |\boldsymbol{\omega}(f, m)|^2 \rangle_J = \frac{1}{J} \sum_{j=1}^{J} |\boldsymbol{\omega}_j(f, m)|^2$$

Hypothesis 2: The amplitudes of the noise modes are assumed to be random. Therefore, their module calculated by method 3 depends on the choice of the vector $\boldsymbol{\omega}_j(f, m)$:

$$\forall\, m \in M_N, \exists\, j \neq j', |\boldsymbol{\omega}_j(f, m)|^2 \neq |\boldsymbol{\omega}_{j'}(f, m)|^2 \quad (32)$$

Hypothesis 3: Let us call m_n the noise mode having the highest mean value

$$\begin{aligned} &\langle |\boldsymbol{\omega}(f, m_n)|^2 \rangle_J \text{ by method 3} \\ &\langle |\boldsymbol{\omega}(f, m_n)|^2 \rangle_J = \frac{1}{J} \sum_{j=1}^{J} |\boldsymbol{\omega}_j(f, m_n)|^2 \end{aligned} \quad (33)$$

This implies the following relation:

$$\forall\, m \in M_N, \exists\, m_n, \langle |\boldsymbol{\omega}(f, m_n)|^2 \rangle_J \geq \langle |\boldsymbol{\omega}(f, m)|^2 \rangle_J \quad (34)$$

The gain in (S/N)G_3 (dB) in method 3 is assumed to be sufficiently large to allow a reduction of each amplitude $|\boldsymbol{\omega}_j(f, m_n)|^2$ ($j = 1, 2, \ldots, J$) for noise mode m_n, such that

$$\langle |\boldsymbol{\omega}(f, m_s)|^2 \rangle_J > \langle |\boldsymbol{\omega}(f, m_n)|^2 \rangle_J \quad (35)$$

where m_s is the acoustic mode with the lowest mean value.

Using this relation and Eqs. (31) and (35), it is possible to write

$$\forall\, m \in M_S, \forall\, j, |\boldsymbol{\omega}_j(f, m)|^2 > \langle |\boldsymbol{\omega}(f, m_n)|^2 \rangle_J \quad (36)$$

In other words, the mean value of any noise mode is assumed to be smaller than the mean value of any acoustic mode. Nevertheless, the amplitudes of all the noise modes are not assumed to be smaller than the amplitudes of all acoustic modes.

Hypotheses 1 [Eqs. (30) and (31)] and 2 [Eq. (32)] show that the sets M_S and M_N can be determined by calculating the variance of the mode amplitudes provided by method 3 [Eq. (25)] on each vector $\boldsymbol{\omega}_j(f, m)$ of $\Psi(f, m)$:

$$\begin{aligned} \sigma_m^2(f) &= \frac{1}{J} \sum_{j=1}^{J} \left| |\boldsymbol{\omega}_j(f, m)|^2 - \frac{1}{J} \sum_{j'=1}^{J} |\boldsymbol{\omega}_{j'}(f, m)|^2 \right|^2 \\ m &= -\frac{J}{2}, \ldots, +\frac{J}{2} - 1 \end{aligned} \quad (37)$$

It is easy to show that

$$\begin{cases} \sigma_m^2(f) = 0 \text{ for } m \in M_S \\ \sigma_m^2(f) \neq 0 \text{ for } m \in M_N \end{cases} \quad (38)$$

It appears that the sets M_S and M_N can be found by performing a simple test on the nullity of $\sigma_m^2(f)$. Nevertheless, $\sigma_m^2(f)$ is never equal to zero in practice, even if the variance on the acoustic mode amplitudes is smaller than the variance on the noise mode amplitudes. In fact, for the acoustic modes, $\sigma_m^2(f)$ depends on 1) the numerical accuracy of the computers and 2) the angular structure of the background noise. If it has a broadband angular spectrum, its modes can corrupt the acoustic mode amplitude in a nonuniform manner. Therefore, the determination of M_S and M_N cannot be conveniently carried out using a simple test on the value of $\sigma_m^2(f)$.

C. Numerical Implementation of the Threshold Method (Method 5)

As mentioned previously, the sets M_S and M_N can be obtained by a threshold method. Equation (36) has to be verified to apply this method. This condition is satisfied if the variations of the acoustic mode amplitudes obtained using method 3 [Eq. (25)] are not too large. Taking into account Eqs. (32) and (36), it is possible to find the two unknown sets by using the following strategy:

$$\begin{cases} \textit{if } \exists\, j, \text{ such as } |\boldsymbol{\omega}_j(f, m)|^2 < \langle |\boldsymbol{\omega}(f, m_n)|^2 \rangle_J, \text{ then } m \in M_N \\ \text{if } \forall\, j, |\boldsymbol{\omega}_j(f, m)|^2 > \langle |\boldsymbol{\omega}(f, m_n)|^2 \rangle_J, \text{ then } m \in M_S \end{cases} \quad (39)$$

In this approach, it is necessary to determine the threshold

$$T_S = \langle |\boldsymbol{\omega}(f, m_n)|^2 \rangle_J \quad (40)$$

The calculation of T_S cannot be done directly since the mean value $\langle |\boldsymbol{\omega}(f, m_n)|^2 \rangle_J$ is generally unknown. However, it is possible to define a minimum threshold value using hypothesis 3 [Eq. (33)]:

$$\begin{aligned} T_{S_{\min}} &= \min\{\langle |\boldsymbol{\omega}(f, m)|^2 \rangle_J \\ m &= -(J/2), \ldots, +(J/2) - 1 \end{aligned} \quad (41)$$

It can be shown from this relation that the threshold $T_{S_{\min}}$ is generally smaller than T_S in Eq. (40). Thus, the set M_S of acoustic modes is completely determined using $T_{S\min}$ instead of T_S. However, the threshold $T_{S\min}$ is not quite suitable for finding all the modes belonging to M_N. Some noise modes may then be processed as acoustic modes in $\boldsymbol{\omega}'_j(f, m)$ [Eq. (29)].

The processing in the threshold method is based on Eqs. (39) and (41). It is built in three steps: the angular Fourier transform of the vectors $W_j(f)$ ($j = 1, 2, \ldots, J$) (Eq. 24) is computed to obtain the vectors $\boldsymbol{\omega}_j(f, m)$; the mean value (Eq. 29) is calculated with the vectors

1) Method 1 (Fig. 3a), modes m_1 and m_2 are well-retrieved with their exact amplitudes. Mode m_3 is totally buried in the background noise. This result is consistent with the theory [Eq. (12)].

2) Method 2 (Fig. 3b) finds three modes with their correct amplitudes, but the amplitude of mode m_3 is of the same level as the noise.

3) Using method 3 (Fig. 3c) the result is slightly better than the previous one, but the mode m_3 level remains quite similar to the highest noise components.

$$\boldsymbol{\omega}''_j(f, m) = \begin{cases} |\mathrm{Re}[\boldsymbol{\omega}_j(f, m)]| + i|\mathrm{Im}[\boldsymbol{\omega}_j(f, m)]| \text{ if } \forall\, j,\ |\boldsymbol{\omega}_j(f, m)|^2 > T_{S\min} \\ 0 \text{ if } \exists\, j \text{ such as } |\boldsymbol{\omega}_j(f, m)|^2 < T_{S\min} \end{cases} \tag{42}$$

The noise mode amplitudes are set to zero in Eq. (42) since their characterization has generally no interest in practice. At last, the wave number spectrum of $Y(f, \theta)$ is obtained by calculating

$$\Phi_S(f, m) = \langle|\boldsymbol{\omega}''(f, m)|^2\rangle_J = \frac{1}{J}\sum_{j=1}^{J} |\boldsymbol{\omega}''_j(f, m)|^2 \tag{43}$$

D. Iterative Threshold Method (Method 6)

The problem of determining a correct threshold T_S can be conveniently solved by an iterative method. Equations (34) and (35) give the basic algorithm of this method in four steps. The first three steps are similar to those described previously in method 5. They initiate the iterative process. At the first iteration, the threshold is given by

$$T_S(1) = \min\{\langle|\boldsymbol{\omega}(f, m)|^2\rangle_J\}$$
$$m = -(J/2), \ldots, +(J/2) - 1 \tag{44}$$

In the fourth step, further values of threshold $T_S(i)$ ($i = 1, 2, \ldots$) are determinated using the mean value $\langle|\boldsymbol{\omega}(f, m)|^2\rangle_J$ of the noise modes found in the third step. Taking into account hypothesis 3 [Eq. (36)] the following threshold is obtained at iteration i:

$$T_S(i) = \max\{\langle|\boldsymbol{\omega}(f, m)|^2\rangle_J\}, \qquad m \in M_N \tag{45}$$

The iterative process is performed on the results of the third step. New noise modes can be found, until the threshold $T_S(i + 1) = T_S(i)$. Due to hypothesis 3 [Eq. (35)], the threshold must remain smaller than the acoustic mode m_S having the smallest PSD. In practice, the number of iterations is much smaller than the number of modes calculated (i.e., the number of microphones).

IV. Numerical Simulations

A. Simulation A

The previous discussions are illustrated by the numerical simulation presented in Ref. 4. An acoustic field $s(t, \theta)$, at a single frequency $f = 1$ kHz, consists in three modes of different amplitudes: 1) $m_1 = +2$ (100 dB), 2) $m_2 = -4$ (90 dB), and 3) $m_3 = +5$ (70 dB).

The background white noise level is 95 dB in each frequency band Δf (here, $\Delta f = 39$ Hz), and at every location θ_j. Mode m_1 is thus 5 dB above the background noise, while modes m_2 and m_3 are, respectively, 5 and 25 dB below it. Wave number spectra are computed in the interval $-12 \le m \le +11$, assuming $J = 24$ measurements points. All the results are computed using $L = 100$ statistical averages.

The spectrum of microphone 1 is displayed in Fig. 2 (the decrease above 1500 Hz is due to the anti-aliasing filter). The wave number spectra obtained at 1 kHz by various methods are shown in Figures 3a–3f.

4) Using method 4 (Fig. 3d), mode m_1 is well-retrieved with its correct amplitude. Mode m_2 clearly appears but its amplitude is wrong, and the mode m_3 is not found at all.

5) The threshold method (Fig. 3e) gives the three modes with their correct amplitudes and the noise is completely canceled except for the noise mode $m = -9$. This mode is not removed in this case because $T_{S\min}$ is too small compared to T_S [see below Eq. (41)].

6) The result in Fig. 3f obtained using method 6 after three iterations is identical to Fig. 3e, but the noise mode $m = -9$ is eliminated by the iterative procedure.

B. Simulation B

It is known that any threshold method has some limits. This is true for methods 5 and 6. Both methods remove noise modes, but they can also remove some acoustic modes, if the background noise is very high, more precisely if the mean value of the acoustic modes is smaller than the threshold. Simulation B corresponds to such a case. It is also used to test the ability of methods 3, 5, and 6 to detect a greater number of modes. There are six acoustic modes at 1 kHz: 1) $m_1 = -10$ (90 dB), 2) $m_2 = -7$ (75 dB), 3) $m_3 = -3$ (100 dB), 4) $m_4 = -1$ (65 dB), 5) $m_5 = +2$ (85 dB), 6) $m_6 = +5$ (70 dB). The background noise is the same as in simulation A. Thus, mode m_3 is the only one above the background noise, while modes m_1, m_2, m_4, m_5, and m_6 are, respectively, 5, 20, 30, 10, and 25 dB below it.

1) Using method 3 (Fig. 4a), five among the six acoustic modes clearly appear with their right amplitudes: $m_1 = -10$, $m_2 = -7$, $m_3 = -3$, $m_5 = +2$, $m_6 = +5$. Mode $m_4 = -1$ is totally buried in the background noise.

2) Method 5 (Fig. 4b) enhances the five previous acoustic modes since several noise modes are cancelled. It is also noticed that mode $m_4 = -1$ has been eliminated, because its mean value $\langle|\boldsymbol{\omega}(f, m_4)|^2\rangle_J$ is smaller than the threshold $T_{S\min}$ found by this method.

3) Using method 6 (Fig. 4c), only the five acoustic modes found by method 5 are left, and all the noise modes are

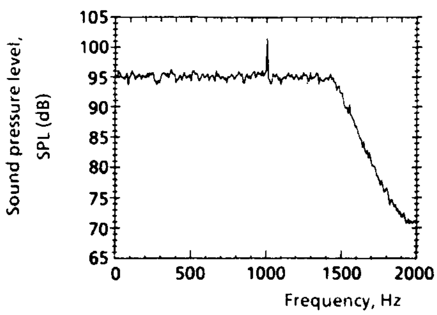

Fig. 2 Numerical simulation with three spinning modes: $f = 1$ kHz, $m_1 = +2$ (100 dB), $m_2 = -4$ (90 dB), $m_3 = +5$ (70 dB). Background noise: 95 dB, $J = 24$ measurement angles, $L = 100$ statistical averages. Synthesized frequency spectrum of the input signal at each microphone angles (resolution $\Delta f = 39$ Hz).

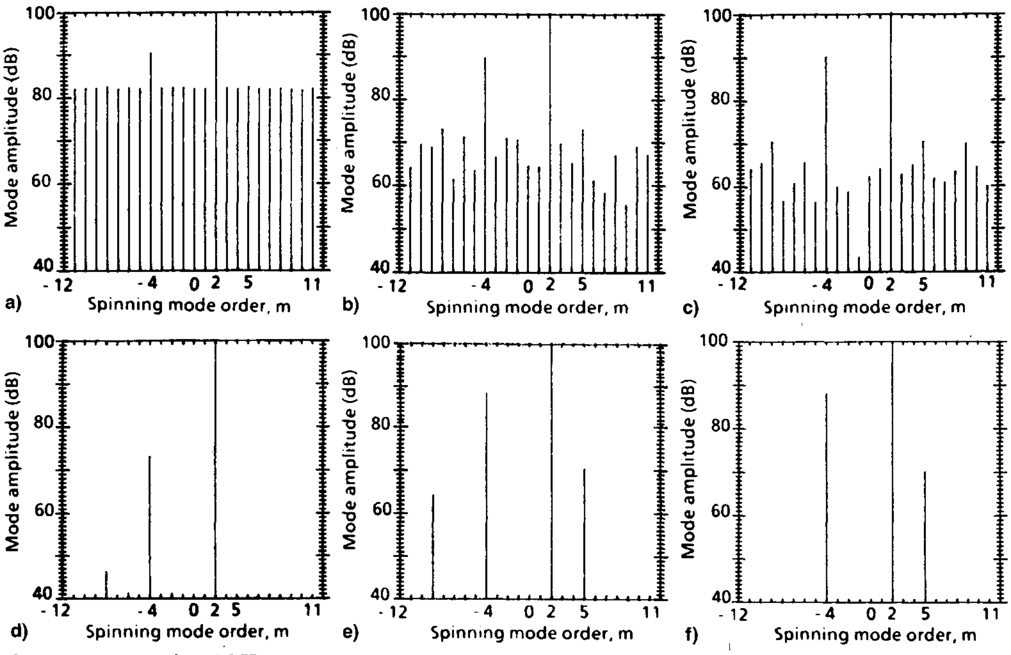

Fig. 3 Wave number spectrum at $f = 1$ kHz corresponding to Fig. 2. Method a) 1, b) 2, c) 3, d) 4, and e) threshold methods 5 and f) 6.

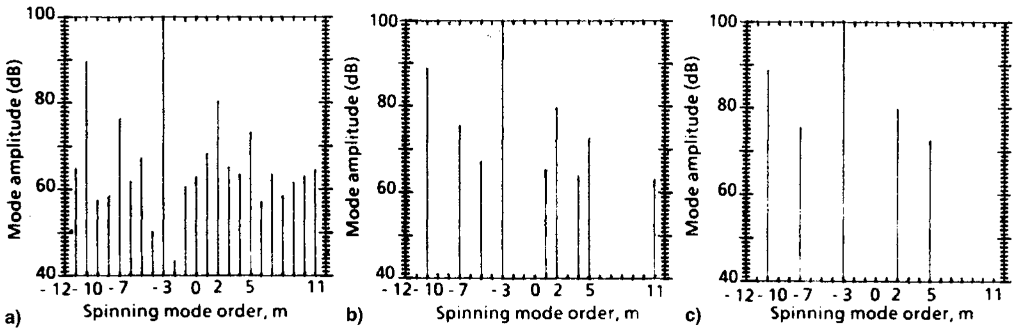

Fig. 4 Numerical simulation with six spinning modes: $f = 1$ kHz, $m_1 = -10$ (90 dB), $m_2 = -7$ (75 dB), $m_3 = +3$ (100 dB), $m_4 = -1$ (65 dB), $m_5 = +2$ (85 dB), and $m_6 = +5$ (70 dB). Background noise: 95 dB, $J = 24$ measurement angles, $L = 100$ statistical averages: a) method 3, b) threshold method 5, and c) iterative threshold method 6.

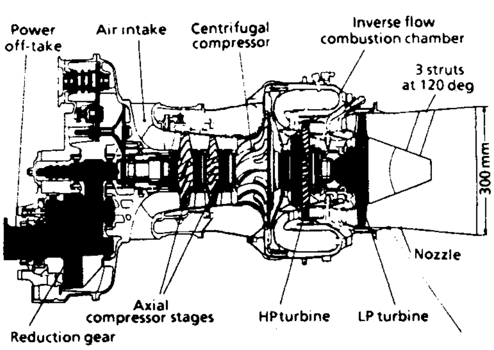

Fig. 5 Schematic view of the Turbomeca TM333 turboshaft engine. Instrumented cross section (see Fig. 6).

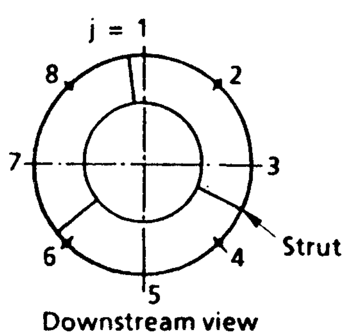

Fig. 6 Locations of the microphones on the TM333 nozzle wall, in the cross section marked in Fig. 5 (the 3 struts every 120 deg are located in a downstream section).

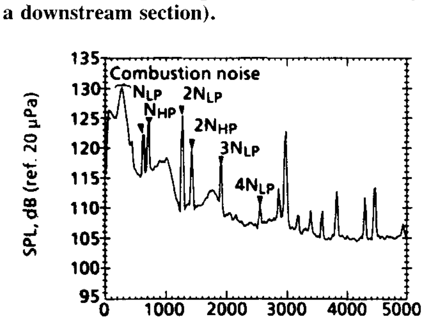

Fig. 7 Frequency spectrum measured by microphone 1 in Fig. 6 (resolution $\Delta f = 39$ Hz).

canceled. Again, mode $m_4 = -1$ is not picked up because the threshold used for the first iteration is the same as the one found by method 5, and this level is too high compared to $\langle |\omega^S(f, m_4)|^2 \rangle_J$.

V. Spinning Mode Analysis in a Turboshaft Engine Nozzle

Methods presented in the previous sections are applied to measurements performed in the Turbomeca outdoor facility at Pau-Uzein.[7] A nozzle cross section of a Turbomeca TM333 turboshaft engine (Fig. 5) was equipped with eight microphones placed every 45 deg (Fig. 6). Additional details on

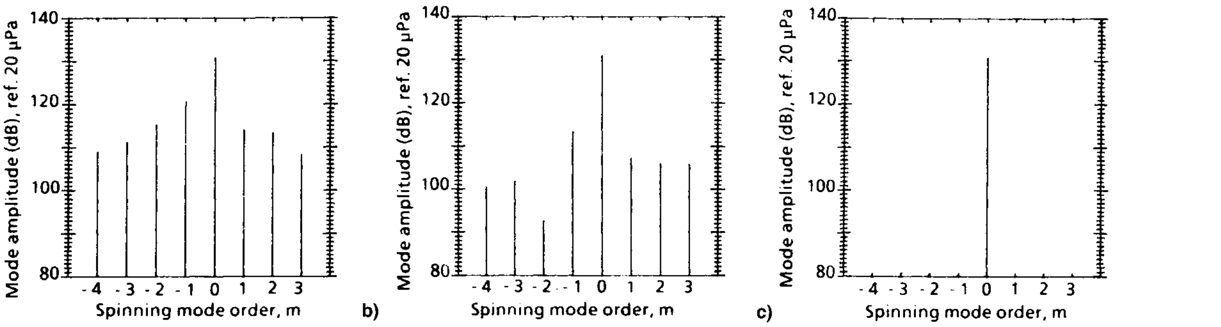

Fig. 8 Wave number spectra in the frequency range of combustion noise, f = 273 Hz (Δf = 39 Hz). Methods a) 1, b) 3, and c) iterative threshold method 6.

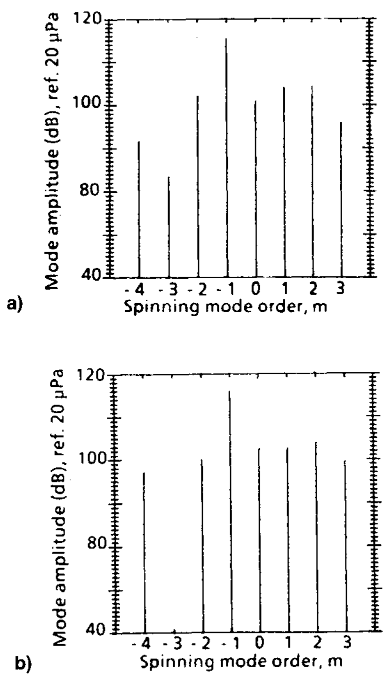

Fig. 9 Wave number spectra at the HP-turbine rotation frequency, $f = N_{HP}$ = 745 Hz (Δf = 39 Hz): a) method 3 and b) iterative threshold method 6.

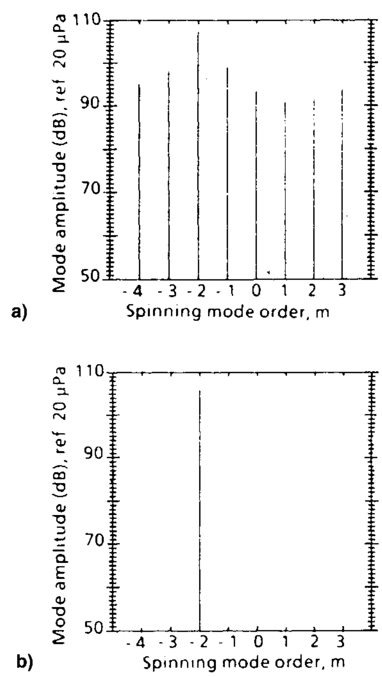

Fig. 10 Wave number spectra at the first harmonic of HP-turbine rotation frequency, $f = 2N_{HP}$ = 1490 Hz (Δf = 39 Hz): a) method 3 and b) iterative threshold method 6.

the experimental setup can be found in Ref. 7. A test at the takeoff power of a twin-engine aircraft (460 kW or 620 hp) is discussed in this section. All the following results are obtained using L = 400 statistical averages.

A. Sound Pressure Level (SPL) Spectrum

The spectrum measured by microphone 1 in the 0–5 kHz (Δf = 39 Hz) frequency range is presented in Fig. 7. The low frequencies (150–400 Hz) correspond to the combustion noise. Tones are harmonics either of the high-pressure turbine rotation speed (N_{HP} = 745 Hz), or of the low-pressure turbine rotation speed (N_{LP} = 627 Hz). Harmonics of the two shaft rotation speeds N_{HP} and N_{LP} appear due to the fact that the turbine stages are transonic, and thus emit multiple pure tones.[8] The main noise source is related to the mean blade aerodynamic loading. Theoretically, only one spinning mode is generated for each tone, and it is equal to the harmonic order f/N (N stands for either N_{HP} or N_{LP}). More precisely, the values of m are positive for the LP-turbine tones and negative for the HP-turbine tones since the two turbine rows are counterrotating.

B. Wave Number Spectra

The wave number spectra are computed for each frequency band Δf = 39 Hz for $-4 \leq m \leq +3$ (i.e., 128 analyses from 0 to 5 kHz). Results are only shown at three frequencies. Data processing is limited to methods 1, 3, and 6 for the first frequency and to methods 3 and 6 for the other two.

Figure 8 shows the analysis at 273 Hz (i.e., at the maximum level of combustion noise). Only the mode m = 0 can propagate at this frequency, which is below the cutoff frequency of the first spinning mode. Using method 1 (Fig. 8a), plane wave m = 0 is about 10 dB above the background noise. Noise level is reduced by 10 dB using method 3 (Fig. 8b). All the modes are removed after three iterations using method 6 (Fig. 8c), except acoustic mode m = 0.

The wave number spectra at the high-pressure turbine rotation frequency, $f = N_{HP}$ = 748 Hz, is displayed in Figs. 9a (method 3) and 9b (method 6). At this frequency the propagating modes are lower than $|m|$ = 2. Results are quite similar by both methods. Mode m = -1 is dominant, and it is about 15 dB above the background noise. Noise modes are not totally removed by method 6. This can be easily explained. The threshold $T_S(1)$ (i.e., the mean value of mode m = -3, which has been eliminated), in the first iteration is too small to give more than one noise mode. Thus, $T_S(1) = T_S(2)$ in the second iteration, and this equality is the condition to stop the iterative process (see Sec. III.D).

Wave number spectra in Fig. 10 are computed to $f = 2N_{HP}$ = 1457 Hz. The background noise remains high in method

3 (Fig. 10a), and the expected $m = -2$ mode (see Sec. IV.A) does not clearly appear. On the contrary, the spinning mode $m = -2$ is the only one left by method 6 (Fig. 10b) after five iterations.

VI. Conclusions

Spinning mode analysis of very noisy acoustic fields requires special methods with highly improved gain in (S/N). Without any treatment, acoustic modes may be overwhelmed by spurious noise modes in the results. Four methods studied in a previous work have been briefly summarized in this article. The method giving the best gain in (S/N) is misleading if the acoustic field contains several spinning modes, because their amplitude may be underpredicted.

A threshold technique is proposed to eliminate this drawback. It first involves an angular Fourier transform of each line of the cross-spectral matrix. Then, the mean values of the modes obtained by the previous step are calculated. Finally, modes with amplitude under a threshold (the lowest of the mean amplitudes) are reduced to zero (noise modes), while the others are coherently averaged (acoustic modes).

The threshold defined above is insufficient for a complete cancellation of the noise modes, because it is generally too low compared to the highest noise modes. This problem is overcome by an iterative method. It consists in deducing, at iteration $(i + 1)$, a new threshold from the noise modes found at the iteration (i). The iterative process is pursued as long as the threshold at iteration $(i + 1)$ is higher than the threshold at the iteration (i). It is stopped when the thresholds are equal at iterations (i) and $(i + 1)$. The quality of the results using this method depends on the threshold $T_S(1)$ determined at the first iteration since the noise having the highest mean value is unknown. $T_S(1)$ has to be sufficiently high for finding several noise modes, and thus, allow to perform more than one iteration. Otherwise, all the noise mode may be not removed.

Numerical tests and experimental results from the TM333 show that the iterative threshold method yields the best result when the above condition is respected.

Acknowledgments

This work was supported by the Service Technique des Programmes Aéronautiques and the Turbomeca Company. The author thanks A. Farrando, P. Jobert, and all the staff of the Turbomeca outdoor facility for their help, which made the tests possible. He also thanks G. Elias and S. Léwy for many fruitful discussions.

References

[1]Mugridge, B. D., "The Measurement of Spinning Acoustic Modes Generated in an Axial Flow Fan," *Journal of Sound and Vibration*, Vol. 10, Sept. 1969, pp. 227–246.

[2]Bolleter, U., and Crocker, M. J., "Theory and Measurement of Modal Spectra in Hard-Walled Cylindrical Ducts," *Journal of the Acoustical Society of America*, Vol. 51, May 1972, pp. 1439–1447.

[3]Harel, P., and Pérulli, M., "Measurement in a Duct of the Space-Structure of Discrete-Frequency Noise Generated by an Axial Compressor," *Journal of Sound and Vibration*, Vol. 23, Aug. 1972, pp. 487–506.

[4]Blacodon, D., and Léwy, S., "Spinning Mode Analysis of the Acoustic Field Generated by a Turboshaft Engine," *Journal of Aircraft*, Vol. 29, No. 6, 1992, pp. 1073–1079.

[5]Bendat, J. S., and Piersol, A. G., *Engineering Applications of Correlation and Spectral Analysis*, Wiley, New York, 1980.

[6]Guédel, A., and Farrando, A., "Experimental Study of Turboshaft Engine Core Noise," *Journal of Aircraft*, Vol. 23, No. 8, 1986, pp. 763–765.

[7]Farrando, A., "Helicopter Turboshaft Engine Acoustic and Infrared Studies and Test," 12th European Rotorcraft Forum, Garmish-Partenkirchen, Paper 87, Sept. 1986.

[8]Benzakein, M. J., Kazin, S. B., and Savell, C. T., "Multiple Pure Tone Noise Generation and Control," AIAA Paper 73-1021, Oct. 1973.